Effect of trough parameters and substrates on the PVDF LB films

A thesis

Submitted in the partial fulfillment of the requirement for the award of degree of

MASTER OF SCIENCE

in

PHYSICS

Submitted by

Ajit Seth

(Roll No. 301604002)

Under the guidance of

Dr. Loveleen Kaur Brar

Assistant Professor

School of Physics and Materials Science

Thapar Institute of Engineering and Technology

June-2018

Certification

I hereby certify that this thesis entitled **"Effect of trough parameters and substrates on the PVDF LB films"** in partial fulfillment for the requirements for the award of Degree of Master of Science in Physics submitted to School of Physics and Materials Science, Thapar Institute of Engineering and Technology, Patiala is an authentic record of my own work and is carried under the supervision of **Dr. Loveleen K. Brar.** The matter submitted via this thesis report has not been submitted for the award of any other degree to the best of our knowledge.

Ajit Seth

Date: 04/8/2018

Ajit Seth

Place: TIET, Patiala

(301604002)

This is to certify that the above statement made by the candidate is correct and true to the best of my knowledge.

Loveleen Kaur Brar

Dr. Loveleen K. Brar

Assistant Professor

Thapar Institute of Engineering and Technology

Patiala- 147004

Dedicated to

My Family and friends

For their love and support

Acknowledgement

First and foremost, I would like to express my sincere and deepest appreciation to my M.Sc. dissertation thesis supervisor, **Dr. Loveleen K. Brar** Assistant Professor, SPMS, Thapar Institute of Engineering and Technology, Patiala- 147004, India for her valuable discussions and suggestions, guidance, strong motivation, encouragement and inspiration throughout my M.Sc. dissertation thesis journey.

I also express my heartiest gratitude to **Dr. Manoj Kumar Sharma**, Head and Professor, School of Physics and Materials Science of Thapar Institute of Engineering and Technology, Patiala-147004, India for his support throughout the period. A special mention to **Dr. Puneet Sharma** and **Dr. Bhupendrakumar Chudasama** for their valuable support.

A special thanks to **Ms. Raveena Choudhary** for her valuable guidance in learning technique.

I am thankful to my encouraging colleagues **Ms. Isha Kalra and Ms. Kaveri Ajravat** for helping me in performing experiments and analyzing the data.

I would like to express my deepest gratitude to my beloved family who has always believed in me, and endured with me during difficult times.

I would like to express my gratitude to my best friends, **Mr. Anurag Yadav, Mr. Deepak Singla, Mr. Kartik Sharma** and **Mr. Shantanu Aggarwal** who inspire me every day to be strong and keep me going with their smile and love.

Last but not least, deepest thanks to all the friends who have always been there with me.

Ajit Seth

Ajit Seth

Date: 04-08-2018

Abstract

Polyvinylidene Fluoride (PVDF) is known to have some very attractive mechanical, electrical and chemical properties. It is being used for parts and applications that require high purity and great mechanical strength. PVDF exists in several crystallized phases such as a nonpolar α-phase, a polar β-phase, a partially polar γ-phase, a partially polar δ-phase, and a nonpolar ε-phase. For various applications, polar β crystals are of critical importance because they show ferroelectric properties. The Langmuir-Blodgett (LB) technique is an effective method for producing thin films of PVDF homopolymer with ferroelectric β phase. In this work, the effect of varying the trough parameters on PVDF homopolymer Langmuir films was studied. These films were fabricated on different types of substrates by the LB deposition method. The changing of compression rate and subphase temperature was reflected on the monolayers as they were characterized using the surface pressure-area isotherms. Initially, the most suitable conditions for the final deposition were the one having a maximum value of static elasticity of solid phase at any specified parameter. The stability of a monolayer at a particular compression rate was confirmed by the cyclic expansion and compression. The oscillating barrier experiment was performed at various values of compression rate and the subphase temperature. This was done to calculate the value of dynamic elasticity of the monolayer and to verify the conditions decided for the final deposition. Finally, the deposition of monolayers was done only for the upstrokes one at a time. For the purpose of depositing multiple layers the process of changing the subphase and dispersing the monolayer was done after the deposition of every layer.

Contents

List of Figures

List of Tables

Chapter 1

Introduction to Polyvinylidene Fluoride Thin Films

1.1 Thin Films

A thin film is defined as a coating of a material (of nanometers to a few micrometers thickness) on a substrate. Its deposition is a self-organizing physical development which depends on the arrangement of discrete molecules or atoms on a substrate depending on the physical conditions. There are many properties which are unfeasible or not easily attainable for the case of bulk matter, so thin films are preferred. Numerous properties of thin films such as optical, electrical, magnetic, chemical, mechanical, & thermal are studied and contribute in developing devices. Additional functionality can also be realized by depositing several layers of different materials. The film thus formed behaves as a completely new engineered material unfamiliar to the bulk form [1].

It can be considered that for the development of material science and engineering field the study of thin film materials is the unifying theme. There are enormous number of studies going on in the area of thin films as there are a huge number of parameters which can be varied giving the resultant film with distinct properties for each change. The inventive and resourceful exploitation of the materials in thin film form have led to massive amounts of achievements in innumerable fields for example electronics, computers, health technologies, laser and fiber optics. The development of the high-performance materials is considered as one of the most significant achievements as the impact of the advances in the area of thin films is so pervasive. Also in order to realize a wide range of real-world service purposes, thin films have been incorporated into engineering systems. These coatings are envisioned to impart a thermal, mechanical, environmental, optical, electrical, magnetic or biological function. In order to progress the speedy improvement of miniature systems, countless steps are taken in the area of thin film technology [2].

The type of substrate used for the deposition process affects the quality of the film. The substrates generally have to be electrically non-interfering, chemically stable and economically feasible. Nature and surface finish of the substrates influences the properties of the deposited film. The film growth and adhesion also depend on the nature of the substrate. A substrate needs to be perfectly clean for the deposited film to be durable. Some substrates such as glass, quartz etc. are found to possess good smoothness and are generally used for the process. The wide variety of substrates that are available can help in examining the behavior of a material.

1.2 Polyvinylidene Fluoride (PVDF)

Polyvinylidene Fluoride (PVDF) is synthesized by the free radical polymerization of vinylidene fluoride as shown in figure 1.2 and is an extremely non-reactive semi-crystalline polymer. PVDF is comparatively very cheap than other polymers. It has been used for applications that require excessive mechanical strength, extraordinary purity and worthy chemical properties such as resistivity to heat and resistance to solvents, bases and acids. It has significantly high flexibility and mechanical strength and is chemically inert. When compared to other polymers, PVDF has a low melting point of 172^0C and has a low density of 1.78g/cm^3. Due to its solubility in polar solvents, it can easily be solution processed. Also, there is no necessity to add stabilizers, processing aids or additives for the melt processing as it has reasonable melting viscosity [3]. Table 1.1 lists some important physical properties of PVDF.

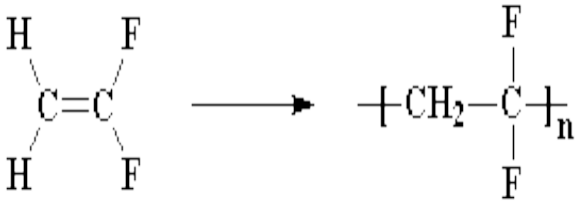

Vinylidene Fluoride poly (vinylidene fluoride)

Figure 1.1 Polymerization of Vinylidene Fluoride

Table 1.1 Physical properties of PVDF

Property	Value
Chemical Formula	$-(C_2H_2F_2)_n-$
Appearance	Whitish or translucent solid
Solubility in Water	Insoluble
Density	$1.78 g/cm^3$
Dielectric Constant	7.2
Volume Resistivity	$>10^{14}$ Ohm-cm
Thermal Conductivity	0.11W/kg m at 23^0C
Melting Point	172^0C

PVDF is an important ferroelectric polymer due to its unique molecular structure and variety of crystalline forms. PVDF has approximately 50% crystallinity and exhibits five different polymorphs: α (phase II), β (phase I), γ (phase III), δ and ε. The α, β, γ and δ polymorphs of PVDF are shown in figure 1.3.

The **α phase** is hexagonal and occurs in a trans-gauche-trans-gauche (TGTG) formation. This formation is a combination of helical and planar zigzag type. The existence of anti-parallel packing of the chains contributes to the para-electricity and non-polar nature of α phase. This phase is one of the most chemically stable states.

The **γ and δ phase** have the conformation of TTTTGTTTG′ and TGTG′ respectively. The δ phase is the polar version of phase having same unit cell but different chain configuration. The γ and δ phases also contribute to the piezo- and pyro-electric properties of PVDF along with the β phase [4].

The **β crystal phase** of PVDF is orthorhombic and forms a planar zigzag or TT where T represents a trans- bond that remains in the same plane as the carbon backbone. The structural investigation concludes the presence of net spontaneous dipole moment in the β phase. This dipole moment is responsible for the piezoelectric, pyroelectric and ferroelectric properties of this phase. It is formed only under special conditions by different techniques such as vapor

deposition of oligomeric PVDF, solution-casting from highly polar solutions, by blending with surface charged nanoparticles or nucleating agents and melt crystallization at high pressure. The β-phase can be achieved by mechanical-stretching and electrical poling of the α-phase at high electric fields under particular temperatures [4].

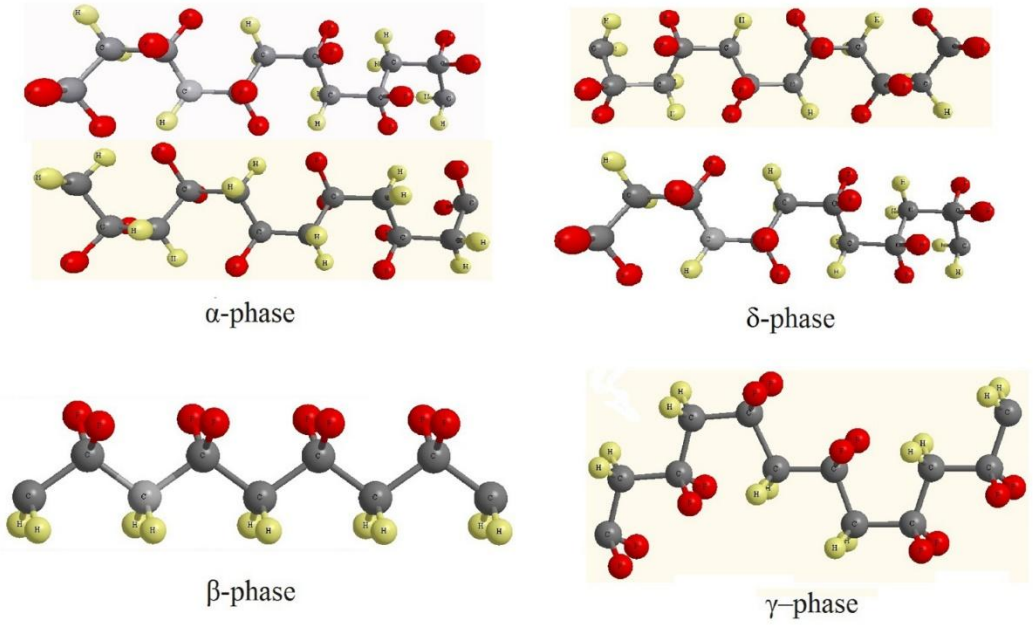

Figure 1.2 Polymorphs of PVDF [5].

1.3 Thin Films of PVDF

Thin films of PVDF are known to have a wide range of applications in devices and are studied due to their beneficial dielectric, ferroelectric and piezoelectric properties. So it's required to obtain β phase in the synthesized PVDF thin films because of the ferroelectric and the piezoelectric properties offered by it. The stretching method is conventionally used to make freestanding β phase PVDF films in which the non-polar α phase films are stretched. But this method cannot be applied to thin films deposited on substrates. The use of copolymers i.e. a polymer having two different kinds of monomers is prominent in many applications. But the homopolymer PVDF films, i.e. polymeric films having the only single type of monomers, are found to have many advantages when compared to the co-polymer counterpart due to greater intrinsic polarization, higher Curie temperature, developed breakdown strength and considerably lower cost [6].

The homopolymer films are perfectly insulating as there is no current leakage which is observed in the case of copolymer films due to crystal defects. These β phase PVDF

homopolymer thin films have a high value of the remanent polarization and hence show excellent ferroelectric properties. The films have higher breakdown strength and flexibility than the copolymer films and are easy to fabricate because of the low processing temperature. This is of great practical application in the field of electronics as the demand for the use of flexible devices is increasing very quickly. The films also are thermally stable in nature due to the high transition temperature of PVDF i.e. about 170^0 C. [7]

1.4 Applications of PVDF Thin Films

Thin films of PVDF have a widespread application:

- Vacuum membrane distillation (VMD) by using PVDF membranes for desalination of water [8].
- PVDF film micro-force sensors are used to measure the strength of fiber bonds [3].
- β phase PVDF films are used to prepare organic spin valve devices [3].
- PVDF thin films are used as the piezoelectric element to design an energy harvesting device [3].
- PVDF membranes are fabricated for the purpose of nerve tissue engineering and show potential applications in the biological field [3].
- The use of PVDF membranes as sensors for capturing lamb waves used in structural health monitoring [9].

1.5 References

1. Donald L. Smith, *Thin-film deposition: principles and practice*, New York: McGraw-Hill, (1995).
2. L. B. Freund, S. Suresh, *Thin Film Materials: Stress, Defect Formation & Surface Evolution*, Cambridge University Press, (2004).
3. Liuxia Ruan et al., *Polymers*, **10(3),** 228, (2018).
4. Chaoying Wan and Christopher Rhys Bowen, *J. Mater. Chem. A*, **5**, 3091-3128, (2017).
5. Ekramul Kabir et al., *Journal of Physics D*: Applied Physics, **50**, 16, (2017).
6. S. Chen et al., *Polymer*, **53,** 1404e1408, (2012).
7. Huie Zhu et al., *J. Mater. Chem. C*, **2,** 6727, (2014).
8. Chengui Sunn, *Poly (Vinylidene Fluoride) membranes: Preparation, modification, characterization and applications*, (2009).

9. V.T. Rathod et al., *Sensors and Actuators A,* **163,** 164–171, (2010)

Chapter 2

Literature Review

Overview

This chapter describes the research papers that were studied for the purpose of literature survey. The first section describes the necessary research papers for the basic understanding of Langmuir Blodgett technique for thin film deposition and the characterizations involved. The second section sheds some light upon the various techniques that are used for the synthesis of Polyvinylidene fluoride (PVDF) thin films. The last section describes the synthesis of PVDF thin films using the Langmuir – Blodgett deposition.

2.1 Deposition of thin films using Langmuir Blodgett Technique

M. B. Biddle et al 1989 [1]. Polar multilayer films were deposited using the Langmuir Blodgett technique. With the use of special deposition procedures, the molecules were forcibly assembled in X or Z manner. Thin films of a polymerizable material called 10, 12-nonacosadiyonic acid was formed for the case of X and Z type deposition, because of the ease with which it gets polymerized upon U-V exposure. In order to study the application of alternate layer another material called 4-octadecyloxy aniline was synthesized. Glancing X-Ray diffractions and electrical characterizations were done in order to check the uniformity of the layers and the pyroelectric measurements respectively.

D. T. Amm et al 1992 [2]. The process of Langmuir Blodgett was used to fabricate thin films of yttrium arachidate up to 200 layers. A thin oxide layer was formed as a result of uniform decomposition of the films above 300^0C. Three characterization techniques namely Rutherford backscattering, X-ray diffraction and laser reflection were performed to determine the crystal structure and stoichiometric composition of the film. The film was characterized in all stages i.e. before, during and after the decomposition process.

N. Matsuura et al 1997 [3]. The fabrication of conducting cadmium oxide thin films was done using a three-step process involving the deposition of CD arachidate film on a substrate using Langmuir Blodgett technique, followed by the ultraviolet ozone (UVO) decomposition

process and annealing of the film between 220 - 300^0C to form CdO. The UVO process removed 90 % of the organic part from the initially deposited Langmuir film. The surface roughness of nanometre-scale was revealed by atomic force microscopy. This resultant lowering of the conductivity of Cdo thin film, when compared to the bulk Cdo, was due to the surface roughness.

J. Collins et al 2006 [4]. The fabrication of mixed monolayers was successfully done using the LB deposition technique. The mixed layer consisted of a nematic liquid crystal and a fatty acid and its behavior was studied by characterizing the deposited film using UV-Visible spectroscopy. The Langmuir Blodgett film produces homeotropic alignment after the inclusion of a liquid crystal. Hence this alignment acts as an important application in the field of optoelectronics.

R. Kaur et al 2012 [5]. The LB technique was used to deposit a monolayer on water surface and then on a quartz substrate. The film formed was of a ferroelectric liquid crystal (FLC) whose stable monolayer was dispersed on the subphase by compression. The deposition was of Y-type and in order to observe the disparity in thickness of the film so formed, 11 and 22 layers were deposited on the substrate. The whole deposition of multilayers of FLC was confirmed by FTIR spectroscopy and the layering was clearly shown by the X-ray diffraction of the film. AFM provided the analyzed details about the morphology of the film.

Katharine L. Harrison et al 2015 [6]. The mechanical properties of graphene oxide and reduced graphene oxide monolayers were examined to study the liquid phase transfer. The values of compressive and shear moduli as a function of surface pressure are obtained by the oscillating barrier measurements. The results from this measurement show that the graphene oxide monolayers act as two-dimensional solids because of a significant amount of shear modulus. While the reduced graphene oxide layers do not show such behavior.

Huaze Zhu et al 2016 [7]. The thermodynamic and structural features of a system composed of a mixture of hexadecanol and a phospholipid 2-dipalmitoyl-sn-glycero-3-phosphoethanolamine (DPPE) are studied. This is done by forming the Langmuir monolayers and transferring them to mica substrates. The deposited films were imaged using AFM with many scan sizes and at different locations. The AFM data indicates the presence of repulsion as well as the attraction between the two different types of molecules which makes the mixture non – ideal.

2.2 PVDF Thin Films – Synthesis and Analyzation

Jiro Sakata et al 1991 [8]. The Electrospray technique (ESP) was used for the preparation for PVDF films with very high orientation. A 0.2 wt. % solution of PVDF was made in dimethylformamide. The PVDF film was formed on a conductive substrate by a two-step process. It involved the passing of solution through a nozzle to which high voltage supply of the order of 8-15 kV was connected and for the solvent to evaporate dry nitrogen was made to flow. The second step involved the transfer to charged solute ions to a grounded conductive substrate. The film was characterized by X-Ray diffraction and IR measurements were also taken. The films so formed had very high pyroelectric coefficients.

Akiyoshi Takeno et al 1991 [9]. The process of vapor deposition was used to fabricate the thin films of PVDF. The polymer PVDF was heated above 300^0C in the crucible leading to its thermal decomposition in a vacuum system. There was no thermal decomposition in order to evaporate the low molecular weight fractions in PVDF as the heating process was done below 300^0C. The deposition on substrates was done below 150^0C and the molecular orientations in the film were parallel to the substrate as β-form was exhibited by the formed films. Piezoelectricity was observed in the formed films.

Xujiang He et al 2006 [10]. The deposition method used for fabrication was spin coating of solutions on silicon substrates. PVDF was dissolved in a mixed solvent having dimethylformamide and acetone in 50:50 volume ratio to prepare 5wt. % solutions. The silicon substrates were previously coated with a layer of aluminum and the spin coating process was done for 20 seconds at the 1000rpm. The process of drying and annealing was done at 100^0Cand 145^0C respectively. The films were characterized by field emission SEM and FTIR.

Venkata Reddy et al 2016 [11]. The fabrication of PVDF was done using the PVDF granules. The granules were dissolved in a polar solvent known as N, N-Dimethyl form amide (DMF) by mixing the different weight percent granules in the solvent. In order to ensure the complete dissolution, the solution was heated at 60^0C and continually stirred. Spin coating was used to prepare stretched thin films on glass substrates at different rates and time. The annealing of the formed film was done at different temperatures to study the effect of annealing treatment. The formed film can easily be characterized for further studies using instruments like FTIR, X-Ray Diffraction (XRD), DSC and Atomic Force Microscopy (AFM).

Monika Haponska et al 2017 [12]. The immersion precipitation method was used to prepare the PVDF membranes. A 15 wt. % homogeneous casting solution was prepared by dissolving the PVDF pallets in N-methyl-2-pyrrolidone and performing continuous stirring for 48 hours. The resulting solution was cooled to around 20^0C after the complete removal of the air bubbles. It was then spread on a glass plate using a casting knife with a set coating speed. It was followed by the complete removal of the solvent by dipping in precipitation bath and a non-solvent bath forming a resultant solid film and the drying process was carried out at 40^0C for 24 hrs. The crystallinity of the formed film was investigated using FTIR and the cross-sectional and surface morphologies by Environmental Scanning Electron microscopy.

2.3 Langmuir Blodgett Deposition of PVDF thin films

Yadong Jiang et al 2007 [13]. The deposition of monomolecular thin films of PVDF was done by LB technique in order to meet the requirement of molecule-based electronic devices. PVDF was dissolved in N, N dimethylformamide with a concentration of 0.1%. The formed films were of Y-type and were deposited on a quartz substrate. A hysteresis loop was achieved as films show polarization even without poling due to the asymmetric structure. The IR spectra obtained was also in accordance with the previously achieved results.

Shuting Chen et al 2012 [14]. The Langmuir Blodgett fabrication of ultrathin PVDF film involved the dispersion of a solution of PVDF, with a concentration of 0.05 wt. % in a solvent of DMF and acetone being 1:1 in volume, on purified water acting as a subphase. The high-quality ferroelectric β phase was directly observed in the film and was confirmed by the XRD pattern and the FTIR spectra. FE-SEM images of the film indicated a dense and homogeneous surface. The results from the Piezoresponse Force Microscopy showed that there was no dipole reorientation in the poling process and hence the film was completely self-polarized.

J. L. Wang et al 2014 [15]. The thin films of PVDF were prepared using the Langmuir Blodgett technique in order to study the electrical properties. The films were deposited on Au-coated Si. In order to improve the crystallinity in the formed films annealing at145^0C was done for 3hours. The β-phase was achieved in the formed films which are ferroelectric in nature and a significant amount of piezoelectricity was also observed by piezoelectric force microscopy (PFM). There were 80 transferred layers and the thickness was the order of 80nm. X-Ray diffraction was used in order to analyze the crystal structure.

Huie Zhu et al 2014 [16]. The quasi-monolayers of PVDF were deposited on Al coated glass surface by the Langmuir deposition technique. The thickness of the film ranged from 12-82 nm depending upon the number of layers deposited. The value of the remanent polarization was observed to increase after a particular thickness to a value of 6.6 μC cm^{-2} (81 nm), which is the highest value ever recorded. The hysteresis loop characterization of the film at different thickness showed that film with the least thickness value was also ferroelectric. This high remanent polarization and such easy fabrication make these films a great asset for non-volatile memory applications.

Huie Zhu et al 2015 [17]. The effect of different solvents on the properties of Langmuir films of PVDF was studied. All the solvents used were polar in nature. The films were deposited using the Langmuir Blodgett technique in order to influence the orientation of the PVDF. The use of different solvents affected the properties in the aggregation state of the molecules at the interface as well as the crystal structure. The monolayers at the air-water interface were analyzed using the Brewster angle microscopy (BAM). The deposited films were characterized using FTIR and AFM.

2.4 References

1. M. B. Biddle et al., *Sensors and Actuators*, **20,** S. 307-313, (1989).
2. D. T. Amm et al., 1992, *Appl. Phys. Lett.*, **61,** 522 (1992).
3. N. Matsuura et al., *Thin Solid Films*, **295,** 260-265, (1997).
4. J. Collins et al., *Thin Solid Films*, **496,** 601 – 605, (2006).
5. Ramneek Kaur et al., *Liquid Crystals*, Vol. **39,** No. 11, 1375–1380, (2012).
6. Harrison, K.L et al, *Langmuir*, **31,** 9825–9832, (2015).
7. Huaze Zhu et al, *Chemistry and Physics of Lipids*, **201,** 11–20, (2016).
8. J. Sakata, M. Mochizuki, *Thin Solid Films*, **195,** 175-184, (1991).
9. Akiyoshi Takeno et al., *Thin Solid Films*, **202,** 30 July (1991).
10. Xujiang He, and Kui Yao, *Appl. Phys. Lett.*, **89,** 112909, (2006).
11. Venkata Reddy et al., *IJATES*, Vol. **4,** March (2016).
12. Monika Haponska et al., *Polymers*, **9,** 718, (2017).
13. Yadong Jiang et al., *Integrated Ferroelectrics*, **88,** 21–26, (2007).
14. Shuting Chen et al., *Polymer*, **53,** 1404e1408, (2012).
15. J. L. Wang et al., Appl. Phys. Let*t.*, **104,** 182907, (2014).
16. Huie Zhu et al., *J. Mater. Chem.* C, **2,** 6727, (2014).
17. Huie Zhu et al., *Soft Matter*, **11,** 1962, (2015).

Chapter – 3

Materials and Methods

Overview

This chapter describes the materials used in the fabrication of thin films and all the procedures required to perform the experiment. Also, the characterization techniques mandatory for the analysis of the designed film are also defined.

3.1 Materials

The following materials were used for the process:

1) **Polyvinylidene Fluoride (-($C_2H_2F_2$)$_n$-):** The PVDF used for the experiment was of 98% purity and bought from Alfa Aesar.
2) **N – Methyl – 2 – pyrrolidone (C_5H_9NO):** It is a powerful, aprotic solvent with high solvency and low volatility. An aprotic solvent is the one that does not contain O-H or N-H bond and hence is incapable of donating a proton. But a polar aprotic solvent can accept H-bonds from other molecules. The interaction of NMP with water has a significant effect on its properties and hence can be used in a variety of processes. NMP has high chemical and thermal stability and is completely miscible with water at all temperatures**.** It was used to dissolve PVDF and disperse it on the surface of the subphase. It evaporates quickly at room temperature. It was a product of Loba Chemi Pvt. Ltd.

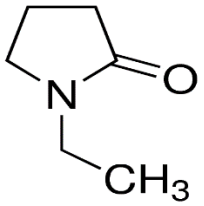

Figure 3.1 Structural formula of N-methyl-2-pyrrolidone (NMP) [1].

3) **Acetone (CH_3COCH_3):** The acetone used was a product of RANKEM with purity greater than 99%.

4) **Methanol (CH_3OH):** The methanol was acquired from the SDFCL (HPLC Grade) and was used for the cleaning of trough and barriers.
5) **Propane-2-ol (C_3H_8O):** It was acquired from Fisher scientific with purity of 99.7% and was used to clean the trough and barriers after cleaning them with methanol.
6) **Deionized Water:** The subphase used for the process was deionized water with a resistivity of 18.2 MΩ and was obtained from Millipore Q3 system. It was also used for cleaning the trough as well as the barriers.
7) **Substrates:** There were three different substrates that were used for the deposition process.
    a) **Glass slides:** Borosilicate slides cut in the size 2.6 cm X 2.6 cm and were a product of borosil. The thickness of slides was 1 mm. The substrates were cleaned by piranha method having sulphuric acid and hydrogen peroxide in 7:3 volume ratio. It was followed by sonication in acetone, methanol and deionized water likewise.
    b) **Mica:** Due to very less contamination and scratch – free surface these substrates are used. It has minimum tendency to crack and is extremely even and smooth. The size of the substrate was 24.90mm X 15.70mm. The thickness was 0.055mm. A layer of mica was removed using a tape and then used for deposition.
    c) **ITO Coated Glass:** Indium Tin Oxide (ITO) coated glass substrates are used for various applications as it has low sheet resistance and high transmittance. The size of the substrate was 12.5mm X 13 mm. The thickness was 1.06mm. These substrates were sonicated in acetone, methanol and deionized water likewise.

3.2 Langmuir Blodgett

A Langmuir film is defined as a floating monolayer which is formed on the surface of a liquid-air interface. The deposition of the Langmuir film on any solid substrate is known as Langmuir – Blodgett deposition. The most critical step in the deposition process is the selection of the substance to be deposited in such way that there is a strong anisotropic interaction between the molecule and the subphase. Generally, the material whose monolayer is to be deposited is amphiphilic in nature [2].

An amphiphilic molecule is the type of a molecule having one end as the water-loving part (hydrophilic) and the other end as the fat-loving part (hydrophobic). Generally, an amphiphilic molecule contains long hydrocarbon chains connected to a polar head. The polar head is what is responsible for the water solubility and the long hydrocarbon tail prevents it. As a result, an insoluble monolayer is formed on the surface of water due to these opposing forces. And the properties of the resultant monolayer can easily be changed by making slight changes in the head or the tail part. When the solution of an amphiphilic substance with any water-soluble solvent is poured on the surface of water then a monolayer of the substance is formed on the surface as soon as the solvent gets evaporated [3].

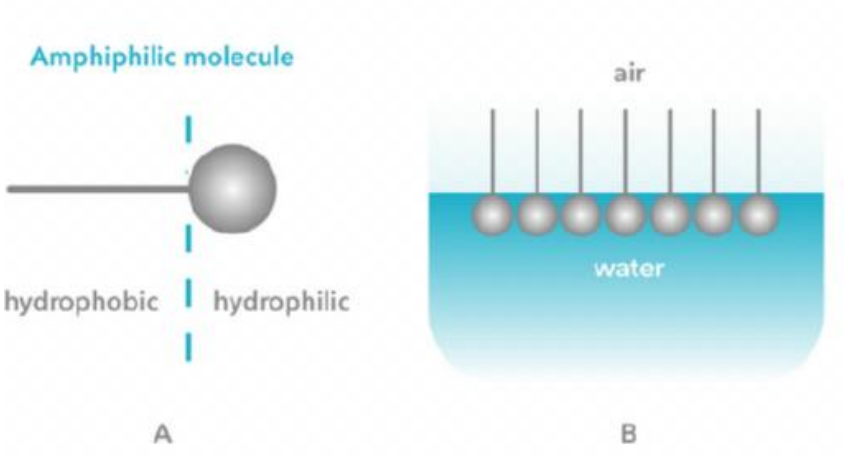

Figure. 3.2 (A) An Amphiphilic molecule; (B) Surface-active molecules [4]

The surface molecules experience a net inward force which is termed as the surface tension (γ) of the liquid. The surface tension surely gets affected by the monolayer of the substance. Hence a quantity known as the surface pressure (π) is needed to be calculated which gives the difference between the surface tension of the pure liquid and the liquid having a monolayer dispersed over it. It is given as

$$\pi = \gamma_0 - \gamma$$

Where γ_0 is the surface tension of the pure liquid and γ is the surface tension of the liquid with the monolayer [3].

3.2.1 Surface Pressure – Area Isotherms

A surface pressure area isotherm is the plot of surface pressure against the area of water surface available to each molecule. The process is carried out at constant temperature and hence the name “isotherm”. Initially, when the value of the surface area is high the molecules are at quite a distance on the surface of the subphase and hence gaseous phase is there. The molecules exert a small amount of force on each other in this case. As the value of the surface area decreases the hydrocarbon chains begin to interact with each other and the phase is called the partially compressed (liquid) phase. Gradually, a stage is reached when there is a transition to a solid-like arrangement of two – dimensional array of molecules. This is seen as the part with an abrupt increase in the slope of the isotherm and hence represents a phase change. The compressibility C is calculated at a constant temperature as [2]:

$$C = -\frac{1}{A}\,(\delta A/\delta\pi)_T;$$

Where ‘A’ is the area and ‘π’ is the corresponding value of the surface pressure. When the value of surface area approaches very small value then the compressibility becomes infinite and a phenomenon known as “collapse” occurs. All the isotherm based research have one basic supposition that the total material in the spreading solution ends up on the surface as a monolayer [5]. A typical surface pressure – area isotherm is shown in figure 3.3.

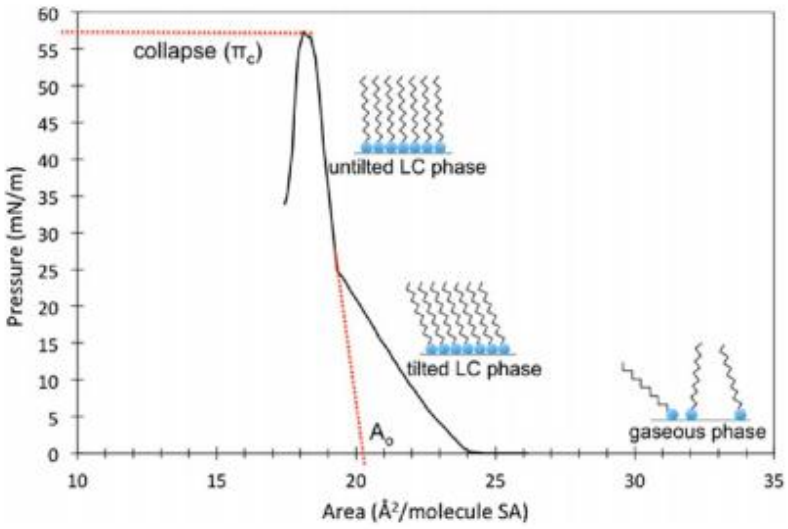

Figure. 3.3 Surface pressure – area isotherm [5].

3.2.2 Experimental Set up of Langmuir – Blodgett Technique

The experimental set – up for the Langmuir Blodgett technique is shown in figure 3.4.

1. Frame: The frame is the module which connects all the other parts to the computer via the layer builder. In order to determine the future upgrades to the system, the frame size plays an important role [7].

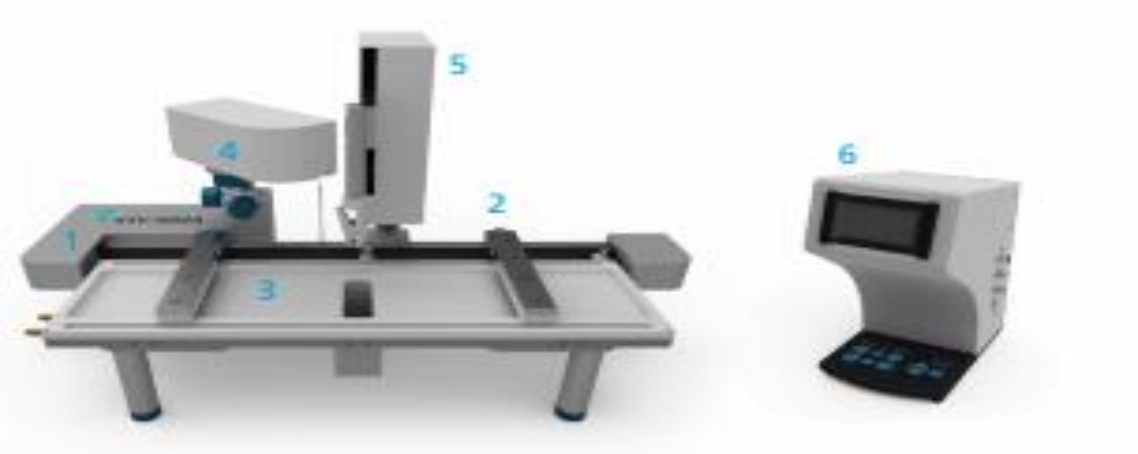

Figure 3.4 Langmuir Blodgett Setup: 1. Frame, 2. Barriers, 3. Trough, 4. A surface pressure sensor, 5. Dipping Mechanism, 6. Layer Builder [7].

2. Barriers: In order to compress the monolayer to designated values barriers are used. The barriers slide parallel to the wall of the trough. Their position is controlled by a software and are hydrophobic in nature to prevent leakage [7].

3. Trough: The trough is made up of Teflon and is hydrophobic in nature. It consists of well in its center for the dipping mechanism in the case of vertical deposition [7].

4. Surface pressure sensor: This sensor consists of a highly sensitive balance which observes the surface pressure. It is done with help of a Wilhelmy plate which measures the interfacial tension at the air-liquid or the liquid-liquid surface shown in figure 3.5. [7].

Figure 3.5 (a) A platinum Wilhelmy plate; (b) Paper Wilhelmy Plate [7]

5. Dipping Mechanism: In dipping mechanism, a solid substrate can be attached to the dipper in a vertical position and the produced film can be obtained on it. Likewise, the dipping rate can also be controlled with a software [7].

6. Layer Builder: This is an interface unit which has an easy to read display and allows simple connections to computers as it is connected via USB. The trough barriers and the dipping mechanism are controlled by it [7].

7. Substrates: The substrates required for the deposition of the thin film can be of two different categories i.e. hydrophilic and hydrophobic. These substrates show different behavior for the deposition of the first layer depending on their types. In the case of hydrophobic ones, the resultant number of layers are even as a monolayer gets deposited even in the first downstroke. While in the case of hydrophilic ones the resultant number of layers is odd as no layer gets deposited in the first downstroke [5].

3.2.3 Film Deposition

When a stable value of pressure as well as temperature is attained in the solid phase then the Langmuir monolayer formed on the surface of the subphase can be deposited on the substrate. Some basic steps that are followed in the deposition process are shown in figure 3.6. The substrate is just smoothly moved inside the subphase surface in both downward and upward fashion. The substrate is placed in the subphase before depositing the film in case of hydrophilic one while it is placed above the surface in the case of hydrophobic one. The deposition process is also affected by various factors such as the rate at which substrate is being dipped or pulled out, the temperature of the subphase, the nature of the solvent and the substrate as well.

There are three different types of ways in which the deposition can occur i.e. X, Y and Z type deposition as shown in figure 3.7.

In the X – type deposition the alignment of the molecule is from head to tail on the substrate and the layer gets deposited only for the down stroke.

In Y – type deposition, the alignment of molecules is from head to head and tail to tail on the substrate and the layer gets deposited for the upstroke as well the down stroke.

In Z – type deposition the alignment of molecules is from tail to head on the substrate and the layer gets deposited for the upstroke only [3].

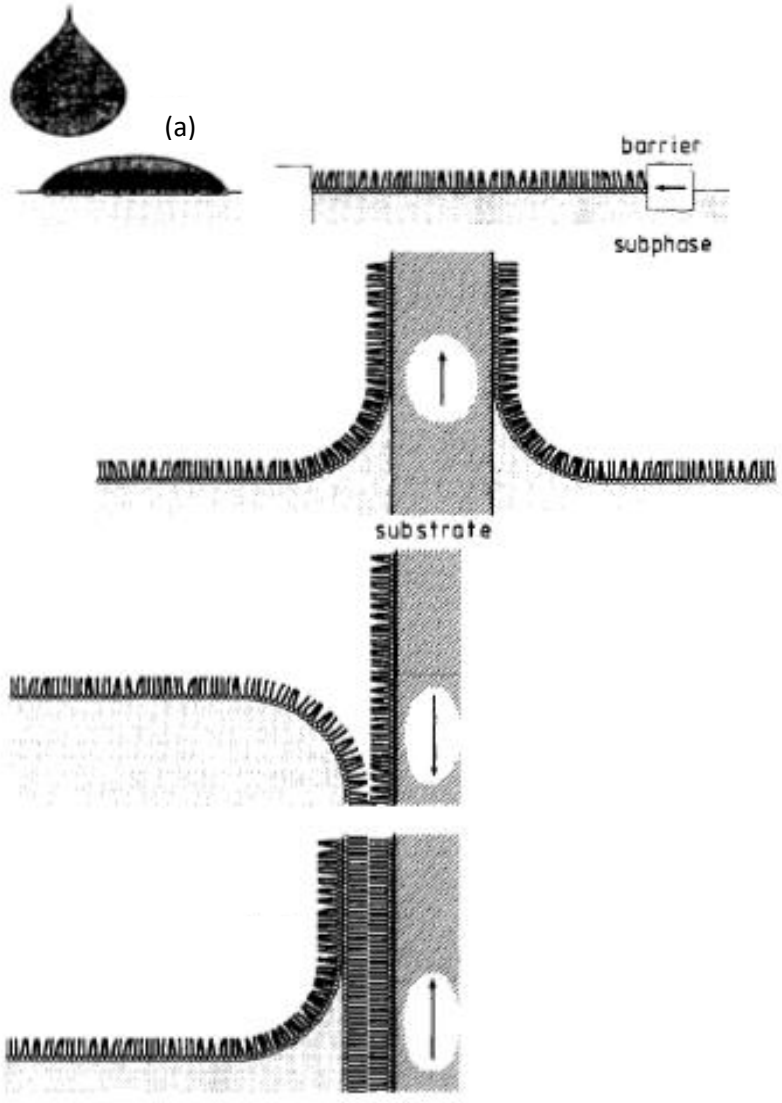

Figure 3.6 Steps in the Langmuir – Blodgett technique: (a) spreading (b) compression (c) transfer of the first monolayer (d) subsequent downstroke (e) subsequent upstroke [5]

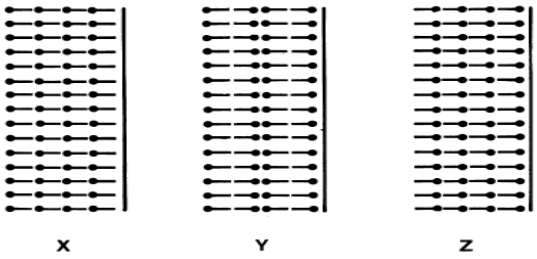

Figure. 3.7 Types of deposition [2].

Transfer Ratio: It's the ratio of the area of monolayer removed from the water surface to the area of a substrate coated by the monolayer. The value of the transfer ratios outside the range 0.95 – 1.05 are an indicator of poor film homogeneity [5].

3.3 Methods

The following procedure was followed to perform the experiments.

3.3.1 Preparation of Langmuir Monolayer

In order to form the monolayer on the surface of the subphase, 0.0936 moles per litre solution of PVDF in NMP was made and 100 microliters of the solution were added drop-wise to the subphase using a microsyringe. The evaporation time for NMP at room temperature is 30 minutes. So, after NMP has evaporated the process of compressing the monolayer was started and isotherms are obtained. The Langmuir monolayers were formed by varying the trough parameters such as the rate of the compression and the temperature of the subphase:

The temperature of subphase was 18^0C for recording the isotherms at 15, 20, 25, 30 and 35 mm/min compression rate.

The rate of compression was 25mm/min for recoding the isotherms at 18^0C, 20^0C, 22^0C and 24^0C subphase temperature.

3.3.2 Deposition of the LB film

The dipping mechanism was used to deposit the monolayer so formed after achieving stability. The dipper speed was selected to be 2mm/min for the upstroke and 15mm/min for the down stroke. The film finally deposited on the substrate is dried out in a vacuum desiccator for 30 minutes. After the process of drying the film is made to crystallize by heating it at a temperature of 145^0C for three hours and then cooled to room temperature [8].

3.4 Characterization Techniques

3.4.1 Surface Pressure – Area Isotherms

A surface pressure-area isotherm is the most fundamental characterization technique for the LB – films. This characterization was carried out for understanding the effect of different parameters such as the rate of compression or the temperature of subphase on the formed films. A brief description of this method is already provided in the section 3.1.1.

3.4.2 Hysteresis

The process of hysteresis is carried out to examine the stability of the film so formed. In this method, the process of compression is carried out followed by an expansion for a particular number of cycles. A typical hysteresis curve isotherm is shown in figure 3.8. If we get reproducible compression and expansion curves then the monolayer so formed can be considered to be a stable one [9].

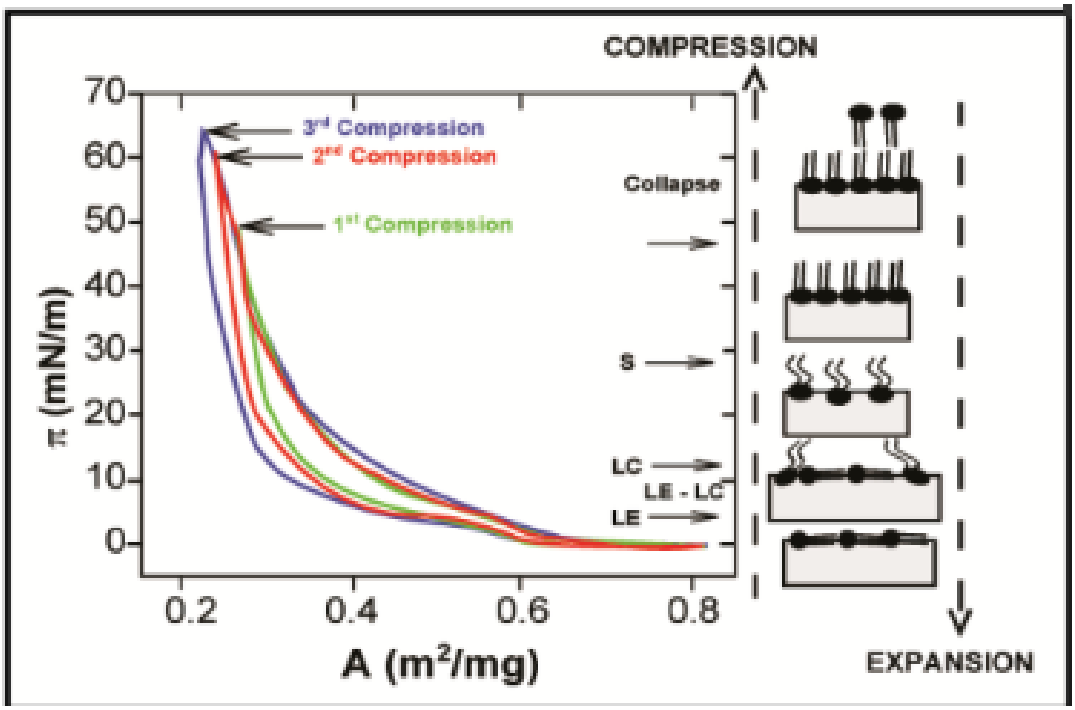

Figure 3.8 Hysteresis curve of an isotherm [10]

The hysteresis isotherms were recorded at 15, 25 and 30 mm/min compression rate at the 18^0C subphase temperature.

3.4.3 Oscillating Barriers

The oscillating barrier is the technique to analyze the viscoelastic properties of the formed monolayer. This is done when the target pressure is achieved. The oscillating barrier mode gives us the value of the most desired value of the surface pressure for the deposition process. We can calculate the values of dynamic viscoelastic properties like the elastic modulus (G), storage elastic modulus (G') and loss modulus (G") at those values of surface pressures at which the phase changes occur [3].

As soon as the target frequency is achieved the barriers start to oscillate as shown in figure 3.9. The relation between all three moduli mentioned above is given as:

$$G = G' + iG''$$

Here, G' is the real part, G" is the imaginary part and G is the resultant complex quantity.

Also, the loss angle is given by the ratio of the loss modulus to storage elastic modulus.

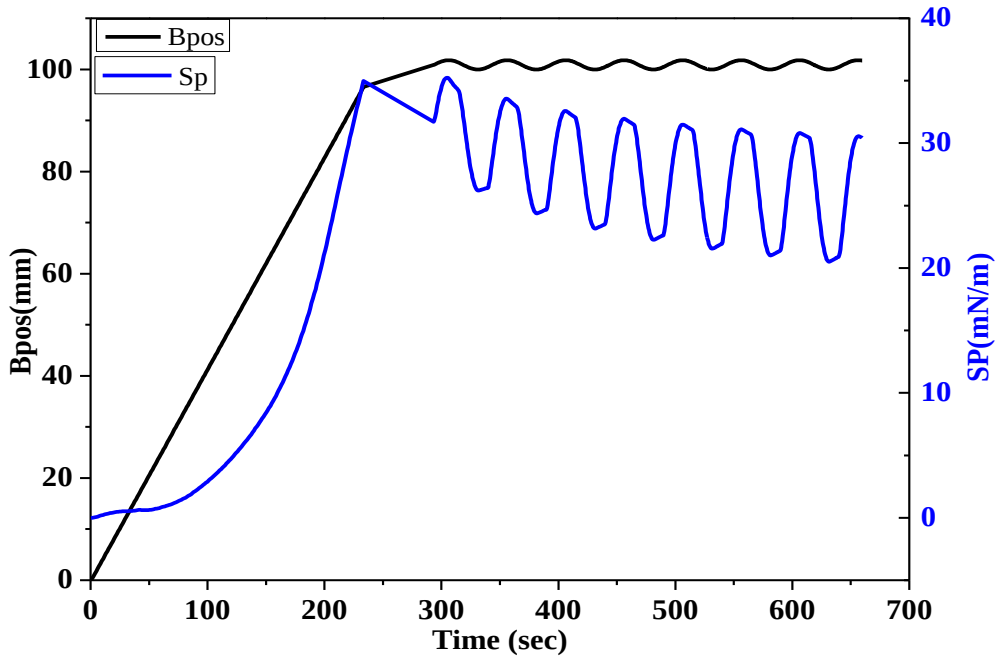

Figure 3.9 Barrier position and surface pressure as a function of time

The oscillating barriers experiment was performed at different:

- Oscillation frequencies (5, 10, 20, 25, 30, 35, 40, 45, 50 and 55 mHz)
- Compression Rates (15, 20, 25, 30 and 35 mm/min)
- Subphase Temperature (18, 20, 22 and 24 ^{0}C)

3.4.4 Atomic Force Microscopy (AFM)

In atomic force microscopy (AFM) a probe is connected at the tip of a cantilever which is placed parallel to the surface of the sample. This probe is very sharp in nature and detects changes in the surface structure of the sample at an atomic scale. The movement of the cantilever is generally detected by a laser beam from a mirror placed at the back of the cantilever and the deflections are sensed using a detector. Furthermore, with the help of

piezoelectric devices, the system is controlled with the detected signal. There are two different modes in which the microscope can work which are constant force mode and constant height mode. The force on the cantilever is generally measured and the mechanical properties of the cantilever are also studied. An image of the surface is obtained by the mechanical movement of the probe in a raster scan of the specimen [11].

The visualization of surface texture and the quantitative measurement of the surface roughness make AFM a perfect method to examine the topography of a deposited film. The surface topography is principally characterized by studying average roughness and the root mean square (RMS) roughness. The RMS roughness measurement is more sensitive to large deviations with respect to the mean line and hence is used to study spatial differences when studying the surface feature using the different scale as well as temporal changes in the creation of a new surface [12].

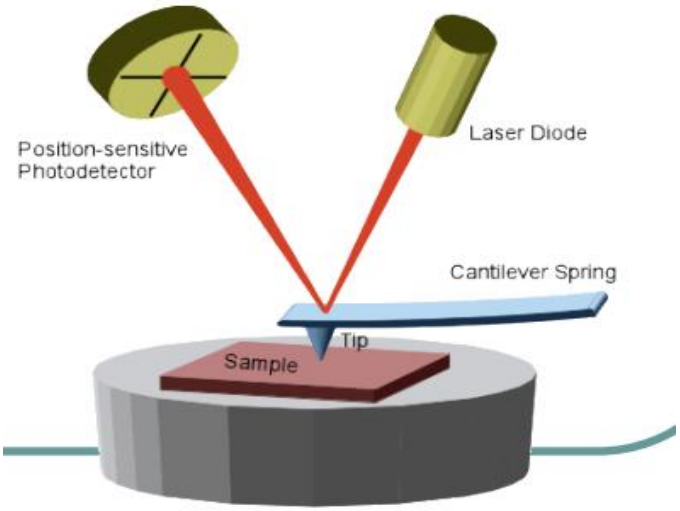

Figure 3.10 Schematic of an Atomic Force Microscope [11]

The AFM imaging is done for different PVDF thin films samples prepared on different substrates in non-contact mode on NT-MDT Solver Next. The topographical view of the surface of PVDF thin film is obtained and rms roughness value is measured.

3.5 References

1. Michael Bader et al**,** *Arch Toxicol*, **81**,335–346, (2007)
2. G. Roberts, Ed. *Langmuir Blodgett films*, plenum press: New York, (1990)

3. Michael C. Petty. *Handbook of Langmuir Blodgett Films*, Cambridge University Press, (1996).
4. Mikkelsen, Alexander. *Experimental Studies of Flow- and Electric Properties of Oil Droplets Including Suspended Clay Particles*, (2012).
5. I R Peterson, *J. Phys. D: Appl. Phys.*, **23,** 379, (1990).
6. Elizabeth C. Griffith et al, *J. Phys. Chem. C*, **117**, 22341−22350, (2013).
7. Manual KSV NIMA Langmuir and Langmuir-Blodgett Deposition Troughs.
8. J. L. Wang et al, *Appl. Phys. Lett.* **104,** 182907, (2014).
9. C. J. L. Constantino et al, *Review of Scientific Instruments* **70,** 3674, (1999).
10. R. Pichot, R.L. Watson, *Int. J. Mol. Sci.*, ***14*(6),** 11767-11794, (2013)
11. PR Khangaonkar, *An Introduction to Material Characterization, Penram Intl. Publishing (India) Pvt. Ltd.-Mumbai*, (2008).
12. Raposo et al, *A Guide for Atomic Force Microscopy Analysis of Soft Condensed Matter. Modern Research and Educational Topics in Microscopy*, **1,** (2007).

Chapter 4

Results and Discussions

Overview

This chapter explains the experimental results obtained from different characterization techniques. The techniques used surface pressure-area isotherms, isotherm hysteresis analysis, oscillating barrier experiments and atomic force microscopy (AFM).

4.1 Surface pressure-area isotherms

In order to get a proper understanding of the elasticity and the phase formation of a Langmuir monolayer formed on the air-water interface, an isotherm plays a vital role. Hence, it is the most commonly used technique to characterize Langmuir monolayers. The value of static elasticity i.e. the value without any dissipative effect can easily be determined from a surface pressure-area isotherm of the monolayer:

$$\mathbf{E} = -\mathbf{A}\,\frac{\mathbf{d\pi}}{\mathbf{dA}} \quad (\mathrm{mN/m})$$

In the present work, all the data is recorded by taking deionized water as subphase and monolayers of 0.0936 moles per litre solution of PVDF in NMP are formed.

4.1.1 Effect of Compression Rate: The Π-A isotherms of PVDF on the surface of deionized water recorded for different compression rates are shown in figure 4.1 (a). Table 4.1 shows the value of the mean molecular area (Mma) of both the phase i.e. solid phase as well as the liquid phase for each isotherm as well as the static elastic constant for the solid phase. The table also contains the values of the mean molecular area (Mma*) and the surface pressure (π*) at which the value of elasticity was recorded. The change in compression rate clearly has a significant effect on the nature of the film so formed. The value of the highest surface pressure that is achieved before the collapse region is different for all the cases as shown in figure 4.1 (a)

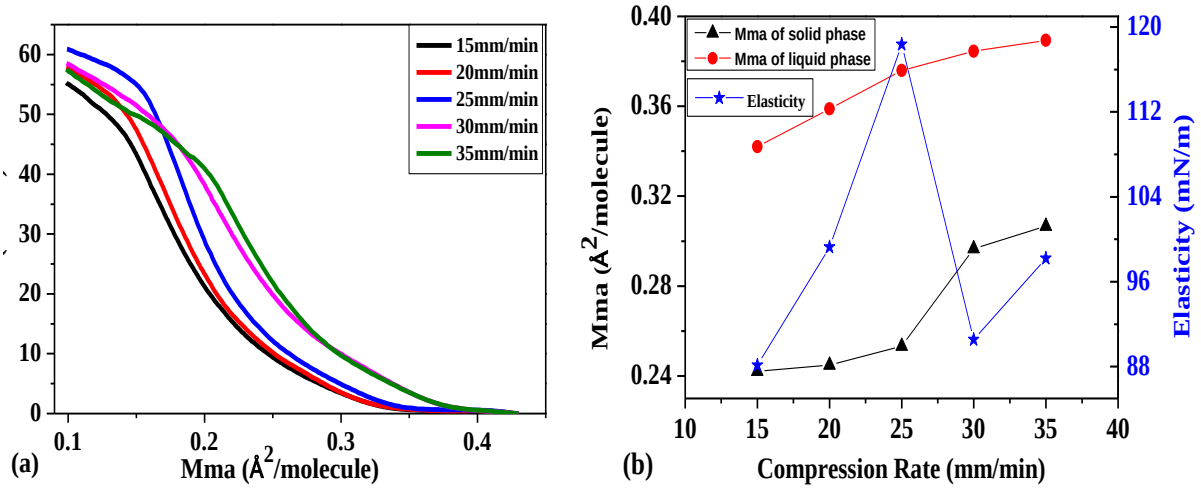

Figure 4.1 (a) π -A isotherms of PVDF on deionized water for different compression rates; **(b)** Variation of Mma of solid and liquid phase and elasticity with compression rate.

Table 4.1 Mma of solid and liquid phases and static elasticity values of solid phase for different compression rates. Mma* and π* are the values at which the elasticity values are recorded.

Compression Rates (mm/min)	Mma of solid phase (Å²/molecule)	Mma of liquid phase (Å²/molecule)	Elasticity (mN/m)	Mma * (Å²/molecule)	π* (mN/m)
15	0.2421	0.3420	88.1237	0.1711	33.859
20	0.2488	0.3588	99.258	0.1753	34.923
25	0.2533	0.3760	118.35	0.1885	37.437
30	0.2967	0.3875	90.5327	0.2056	36.361
35	0.3067	03894	98.189	0.2284	30.027

With the increase in compression rate, the transition from the gaseous phase to the liquid phase is achieved for higher Mma indicating that the condensed phase has a lower density. And this variation is observed for the transition from the liquid phase to the solid phase also. From figure 4.1 (b) it is clear that the increase in compression rate results in higher Mma for solid as well as liquid phase. This is because the area available for the molecules to interact with each other becomes less for a faster compression rate and hence there is a quicker interaction between the molecules leading to the transition of phases. The variation in static elasticity values of the solid phase with compression rate is also shown in figure 4.1 (b). Initially, when the compression rate is low there is not sufficient amount of interaction

between the molecules and this is directly reflected on the corresponding elasticity value. The value of elasticity is obtained highest for 25 mm/min compression rate indicating that this is the most suitable for the further process. When the value of compression rate is higher than this, there is significant amount of repulsion between the molecules leading to a low value of elasticity. So an optimum amount of compression rate is required for getting the highest elasticity value. The collapse value is also highest for 25 mm/min compression rate indicating the highest elasticity. Hence the monolayers will be deposited at the compression rate of 25 mm/min.

4.1.2 Effect of Subphase Temperature: The Π-A isotherms for different subphase temperature are shown in figure 4.2 (a). The table 4.2 gives all the details about the mean molecular area of the phases and static elasticity values for each isotherm.

Table 4.2 Mma of solid and liquid phases; and static elasticity values for different subphase temperature. Mma* and π* are the values at which the elasticity values are recorded.

Subphase Temperature (°C)	Mma of solid phase (Å^2/molecule)	Mma of liquid phase (Å^2/molecule)	Elasticity (mN/m)	Mma * (Å^2/molecule)	(π*) (mN/m)
18	0.2467	0.3234	88.1612	0.1707	31.99
20	0.2146	0.2900	116.59	0.1648	33.42
22	0.1968	0.2700	83.8375	0.1346	36.3831
24	0.1827	0.2560	84.4023	0.1239	33.6386

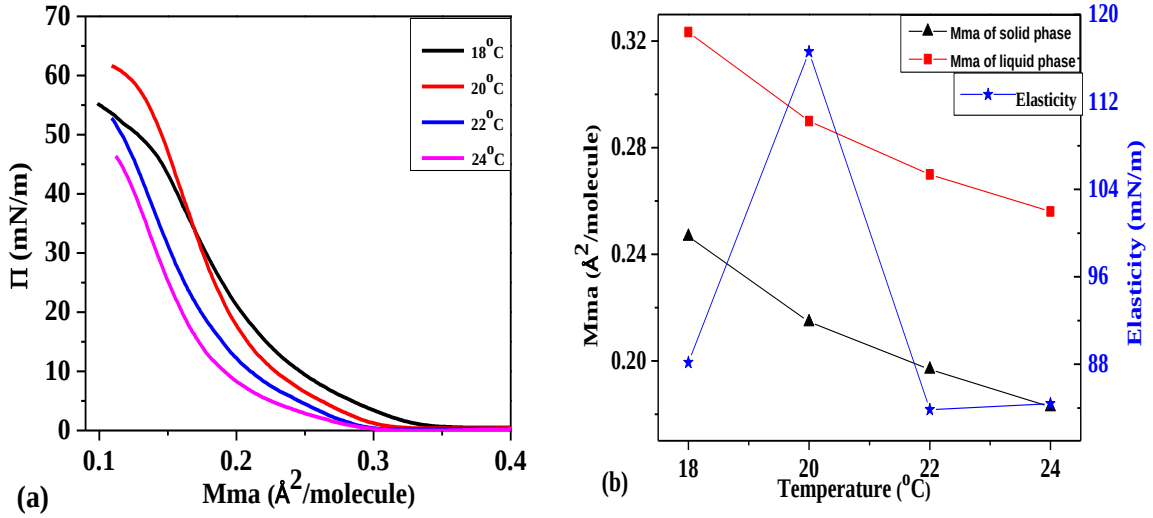

Figure 4.2 (a) π -A isotherms of PVDF on deionized water at different subphase temperature; **(b)** Variation of Mma of solid and liquid phase and elasticity with subphase temperature.

The change in subphase temperature gives distinctive isotherms. It can be inferred from figure 4.2 (a) that with the increase in the subphase temperature the corresponding phase transitions are attained at lower Mma. The decrease in the values of Mma can be observed in figure 4.2 (b). When subphase temperature is increased more thermal energy gets imparted to the system leading to an additional molecular motion at the surface. This allows for the molecules to achieve the best configuration within the monolayer leading to compaction at high temperatures. This decrease in Mma is not reflected in the variation of static elasticity values for the solid phase. At low temperature, the film is too loosely bound so has low elastic constant. But at high temperatures the elasticity decreases again. It is believed that this decrease is reflection of overall decrease in the interaction due to repulsion between the neighbouring monomers as result of compaction. The value of elasticity is highest for 20 °C as is visible in 4.2 (b) indicating the most stable configuration. As the value of temperature is further increased the molecules become very unstable and there is very less interaction between them. So the subphase temperature is taken to be 20 $^{\circ}$C for further process.

4.1.3 Hysteresis: The recurring compression and expansion cycles of the monolayer gives the hysteresis isotherms. In order to know about the stability of a system to maintain a particular configuration hysteresis isotherms are plotted. The hysteresis curves are recorded for three different compression rates i.e. 15, 25 and 30 mm/min. The curves for the case of 25 mm/min are shown in figure 4.3. Table 4.3 contains the mean molecular area of phases of each cycle for all the compression rates. Table 4.4 contains the static elasticity values for each cycle at different compression rates. The variation of parameters is shown in figure 4.4.

Table 4.3 Mma of phases of compression cycles at different compression rate.

Cycle No.	**Compression Rates**					
	15 mm/min		**25 mm/min**		**30 mm/min**	
	MMA_S ($Å^2$/molecule)	**MMA_L ($Å^2$/molecule)**	**MMA_S ($Å^2$/molecule)**	**MMA_L ($Å^2$/molecule)**	**MMA_S ($Å^2$/molecule)**	**MMA_L ($Å^2$/molecule)**
1	0.2437	0.3099	0.224	0.2748	0.2984	0.3707
2	0.2020	0.2455	0.2199	0.2638	0.2546	0.32
3	0.1956	0.2451	0.2076	0.2557	0.2513	0.3159
4	0.1935	0.2089	0.1993	0.2542	0.2447	0.2918
5	0.1907	0.2009	0.1915	0.2436	0.2387	0.2748

Table 4.4 Static Elasticity of compression cycles at different compression rate.

No. of Cycle	Compression Rates		
	15 mm/min	**25 mm/min**	**30mm/min**
	Elasticity (mN/m)	**Elasticity (mN/m)**	**Elasticity (mN/m)**
1	104.658	88.702	109.509
2	157.953	103.24	203.59
3	191.126	104.638	220.66
4	214.187	124.132	239.043
5	217.031	323.886	254.011

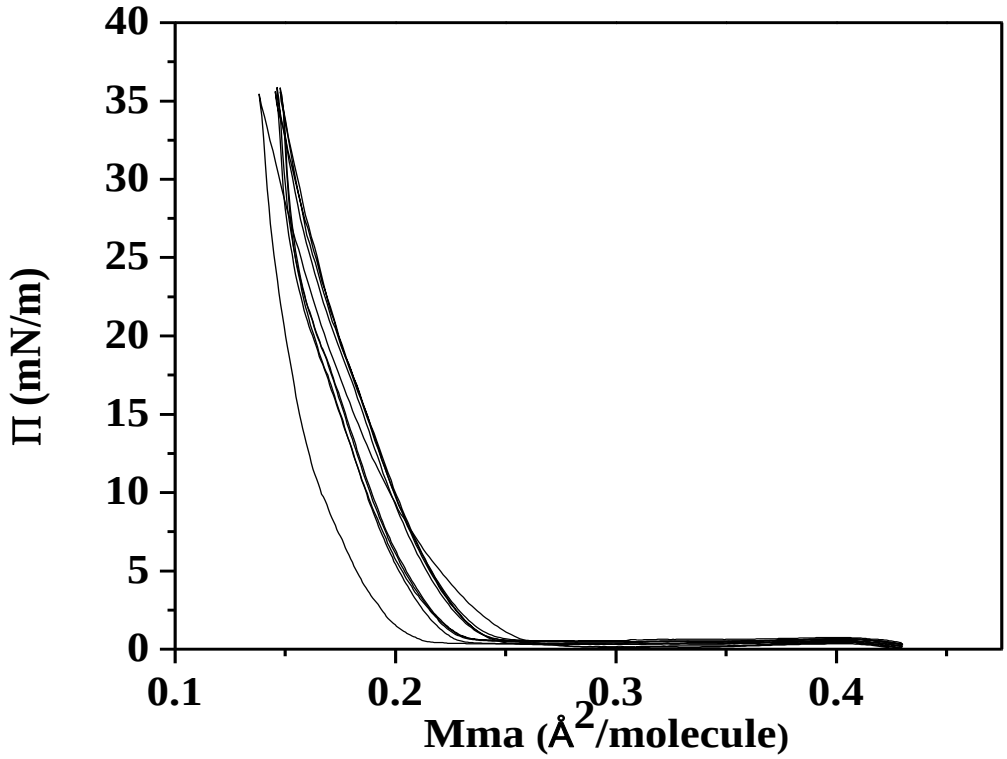

Figure 4.3 Surface pressure-area hysteresis isotherms of PVDF at 25mm/min compression rate.

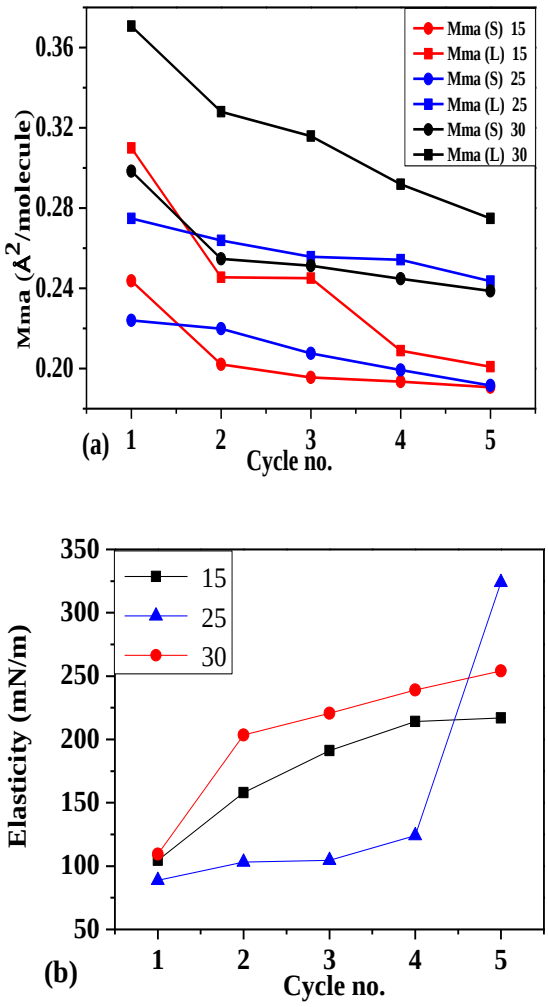

Figure 4.4 (a) Variation of liquid phase and solid phase with cycle no. for barrier speed (15, 25 and 30) mm/min, (b) Variation of static elasticity with cycle number for different barrier speeds (15, 25 and 30) mm/min.

The data for all the three different compression rates shows that with each succeeding cycle there is compaction in the monolayer. The value of Mma steadily decreases with each consecutive cycle for all the cases as visible in figure 4.4 (a). It is clearly visible from the data for all the three cases that the value of elasticity increases for every subsequent cycle. This is because of the reason that with each repeating cycle the monolayer is becoming more compact. It can be inferred from the figure 4.4 (a) that the value of Mma remains most stable for the compression rate of 25 mm/min. Also, it is clearly visible in figure 4.4 (b) that the monolayer has achieved the most stable configuration for 25 mm/min compression rate when compared to others as the value of elasticity is only slightly changing for initial cycles. The sudden increase in the value of elasticity for the last cycle may specify the presence of a some highly favorable configuration. Hence the compression rate of 25mm/min is preferred over the other rates.

4.2 Oscillating Barrier

The interaction forces and the relaxation processes inside a film are studied by measuring the dynamic elasticity. The determination of the dynamic elasticity of a monolayer is done using the oscillating barrier measurement. In order to study the dynamic elasticity values of the monolayers of PVDF on the surface of the deionized water, the monolayer is compressed at the rate of 25mm/min for forming the isotherm. The oscillating barrier measurements are taken at the surface pressure of 35mN/m when the monolayer is in the solid phase. An inbuilt software which exists in the LB trough system is used to determine the values of the Elastic modulus (G), Storage modulus (G') and Loss modulus (G"), which all together are the dynamic viscoelastic properties.

4.2.1 Effect of Barrier Oscillation Frequency

The measurements involved in the barrier oscillation technique are dependent over the time scale on which they are being taken. This is because of the contribution of relaxation processes to the dynamic elasticity. If the speed of the wave generated due to the oscillations is too fast when compared to the barrier speed then the relaxation processes will not be apparent. Also, the speed of the barriers must always be smaller than that of the wave which as a result sets some limits on the frequency. The range of frequency for the oscillation of barriers is taken from 5 mHz to 55 mHz. The compression rate and the temperature of subphase are taken to be 25 mm/min and 20^0C respectively, due to the highest static elasticity values. Table 4.5 shows the values of dynamic viscoelastic properties obtained from the surface pressure variations in figure 4.5. Figure 4.6 shows the variation of the dynamical viscoelastic properties with the frequency of oscillation.

Table 4.5 Dynamic viscoelastic properties obtained at different frequencies.

Frequency (mHz)	**|G| (mN/m)**	**G' (mN/m)**	**G" (mN/m)**
5	234.29	200	121.53
10	214.12	96.94	190.02
20	164.4	92.88	135.65
25	191.54	48.71	185.24
30	325.31	22.15	324.56
35	108.81	67.3	84.7
40	197.06	99.52	134.18
45	238.35	34.3	238.87

50	524.2	235.74	468.2
55	1014.05	289.16	971.95

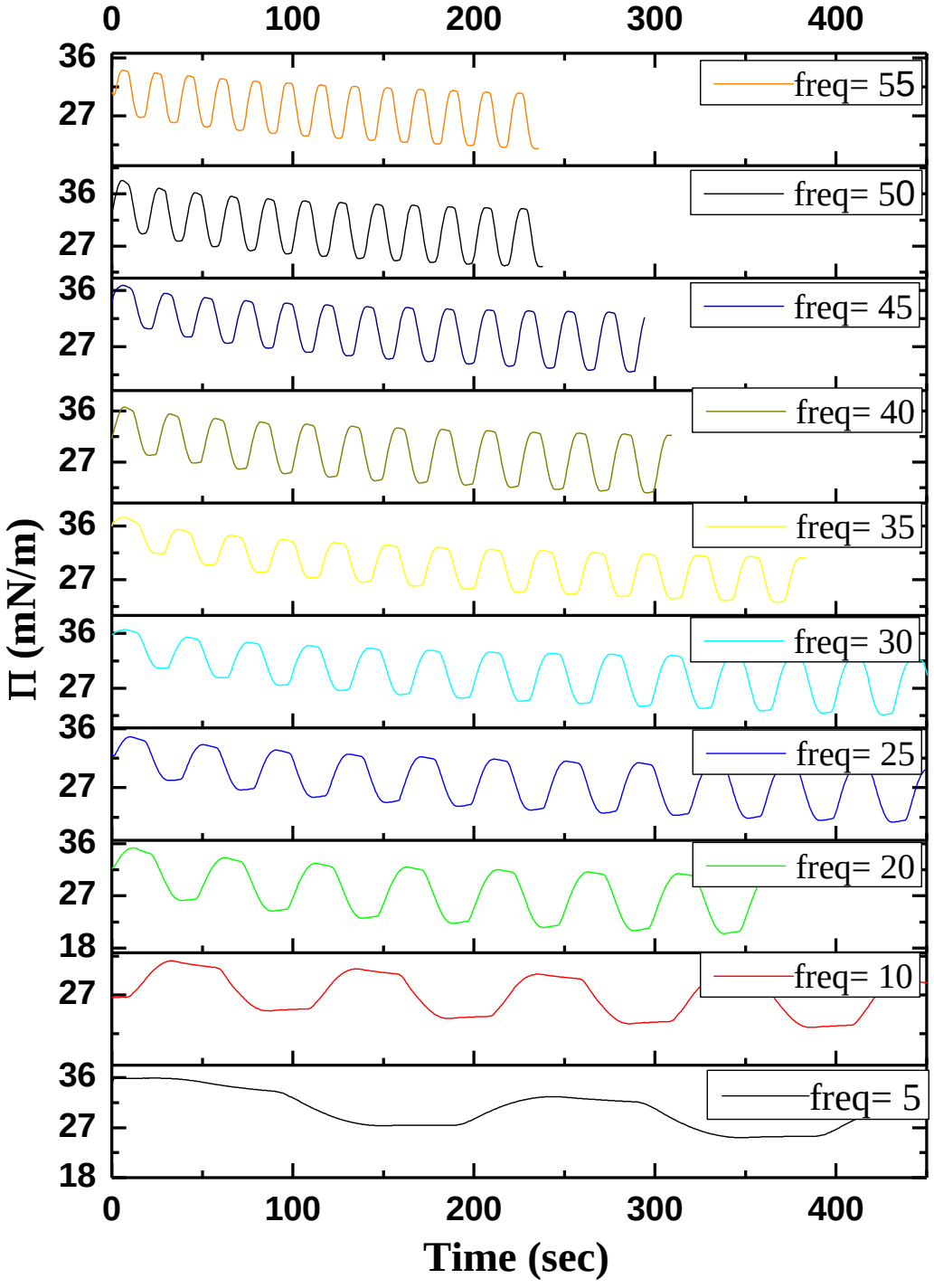

Figure 4.5 Surface pressure variations for barrier oscillations at different frequencies.

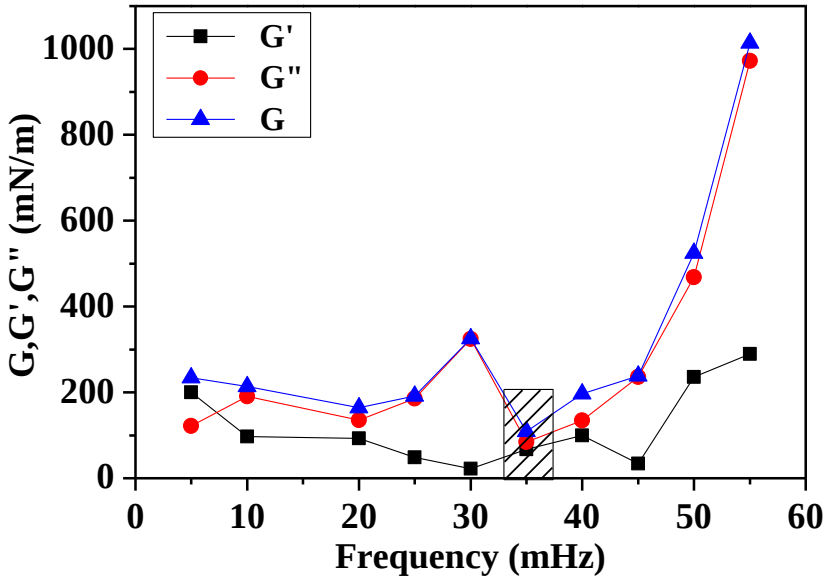

Figure 4.6 Variation of G, G", G" with frequencies of oscillation

The dynamic elasticity modulus slowly decreases with increasing frequency and a sudden increase is observed at 30 mHz. Although the value of dynamic elasticity modulus is higher at this peak the system is not stable as the value of dissipation (G") is also very high. The highest peak of the elasticity modulus is obtained at 55 mHz but with the highest value of dissipation also. It can be concluded from the graph that for 35 mHz the value of dissipation is least and the system is the most stable. So, for the process of observing the effect of compression rate and subphase temperature on dynamic elasticity the frequency for barrier oscillation is chosen as 35 mHz.

4.2.2 Barrier Oscillation at varied compression rates

The varied values of static elasticity of all the surface pressure-area isotherms for different compression rates clearly specify that the elastic properties of the PVDF monolayer are affected by changing the compression rate. For an extended consideration about the dependence of viscoelastic and elastic properties on the compression rates, the barrier oscillation measurements are taken. The experiments are performed at a frequency of 35 mHz for all the compression rates i.e. 15, 20, 25, 30 and 35 mm/min. Table 4.6 shows the values of dynamic viscoelastic properties obtained from the surface pressure variations in figure 4.7. Figure 4.8 shows the variation of the dynamical viscoelastic properties with compression rates.

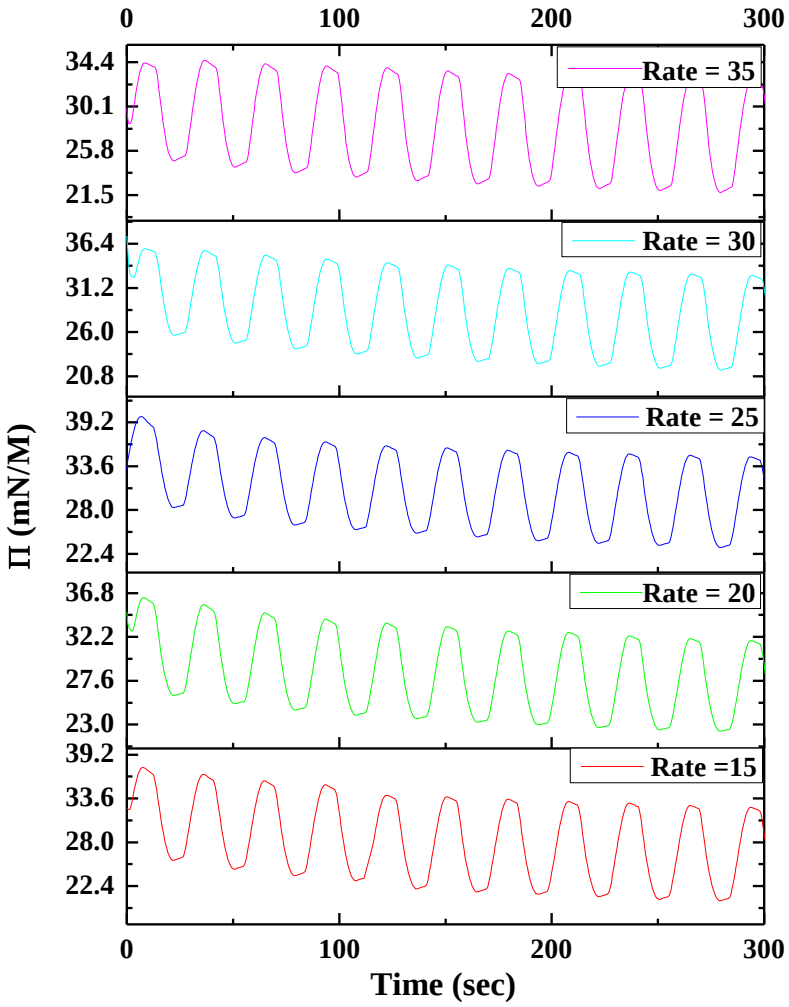

Figure 4.7 Surface pressure variations for barrier oscillations at different compression rates.

Table 4.6 Dynamic viscoelastic properties obtained at different compression rates.

Compression Rates (mm/min)	|G| (mN/m)	G' (mN/m)	G" (mN/m)
15	39.41	161.19	156.3
20	37.71	129.85	124.25
25	52.83	167.55	159
30	472.09	875.3	373.08
35	106.84	151.96	108.07

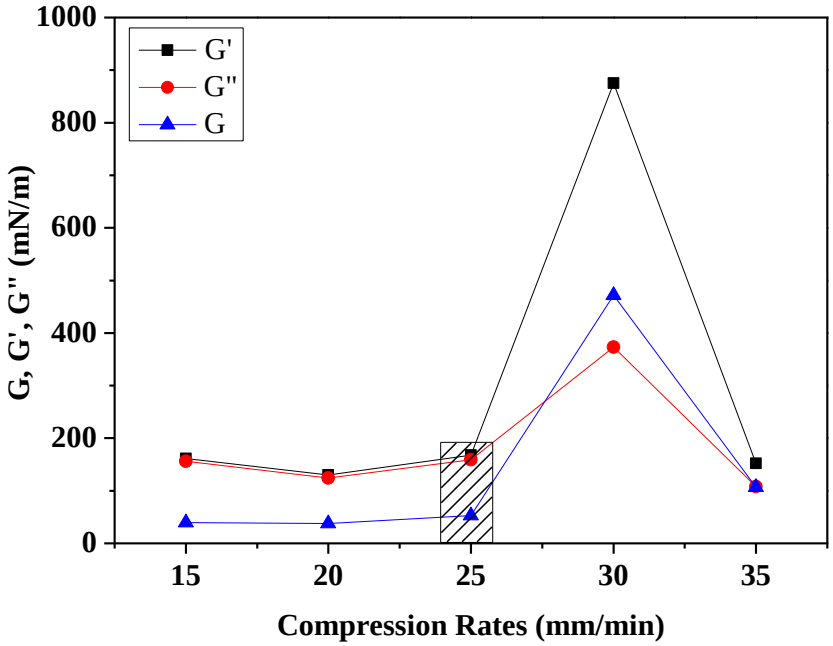

Figure 4.8 Variation of G, G', G" with compression rates.

The compression rate of 25 mm/min is selected as the final rate for the deposition process as there is a low value of dissipation for this rate as shown in figure 4.8. And it is also obtained as the best rate from the static elasticity values and hysteresis curve for the process.

4.2.3 Barrier Oscillation at varied subphase temperature

The mixed values of static elasticity of all the surface pressure-area isotherms for different subphase temperatures evidently specify that the elastic properties of the PVDF monolayer are affected by changing subphase temperature. For a prolonged consideration about the dependence of viscoelastic and elastic properties on the subphase temperature, the barrier oscillation measurements are taken. The experiments are performed at a frequency of 35 mHz and for all the different subphase temperatures i.e. 18 ^{0}C, 20 ^{0}C, 22 ^{0}C and 24 ^{0}C**.** Table 4.7 shows the values of dynamic viscoelastic properties obtained from the surface pressure variations in figure 4.9. The figure 4.10 shows the variation of the dynamical viscoelastic properties with compression rates.

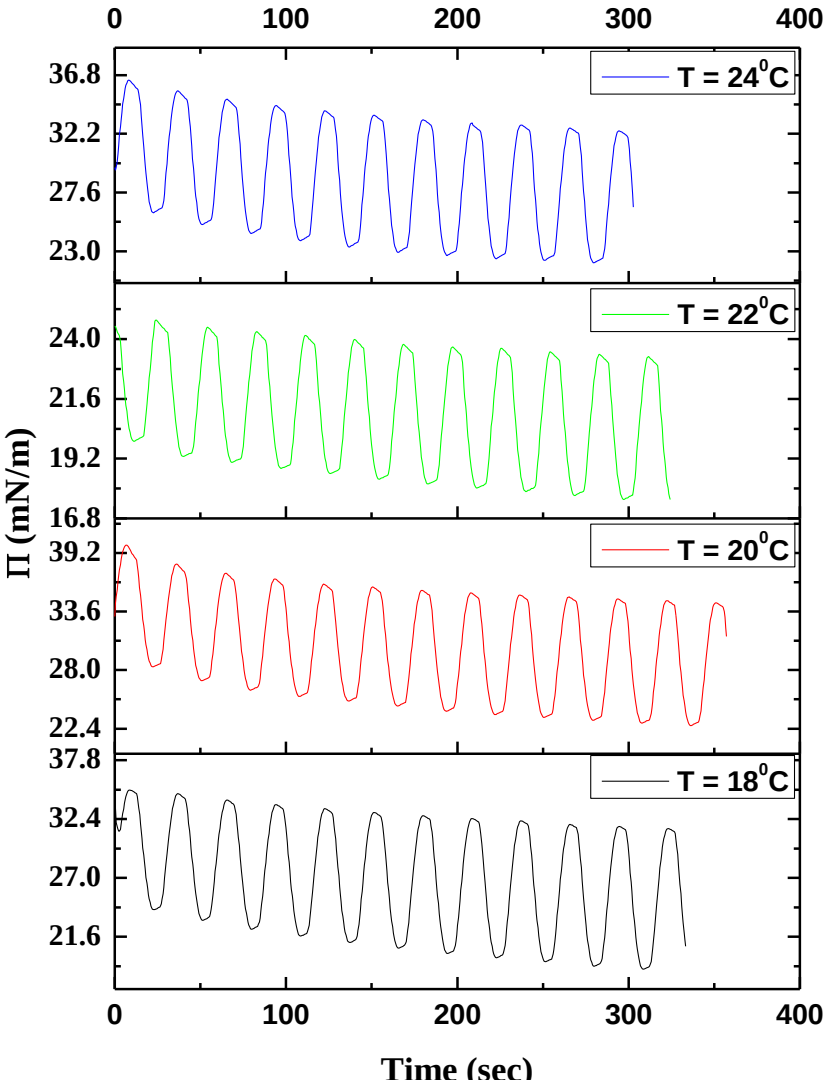

Figure 4.9 Surface pressure variations for barrier oscillations at different subphase temperatures.

Table 4.7 Dynamic viscoelastic properties obtained at different subphase temperatures.

Subphase Temperature ^{0}C	|G| (mN/m)	G' (mN/m)	G" (mN/m)
18	201.68	200.65	20.34
20	167.55	159	52.83
22	81.3	72.81	36.18
24	123.6	121.63	22.08

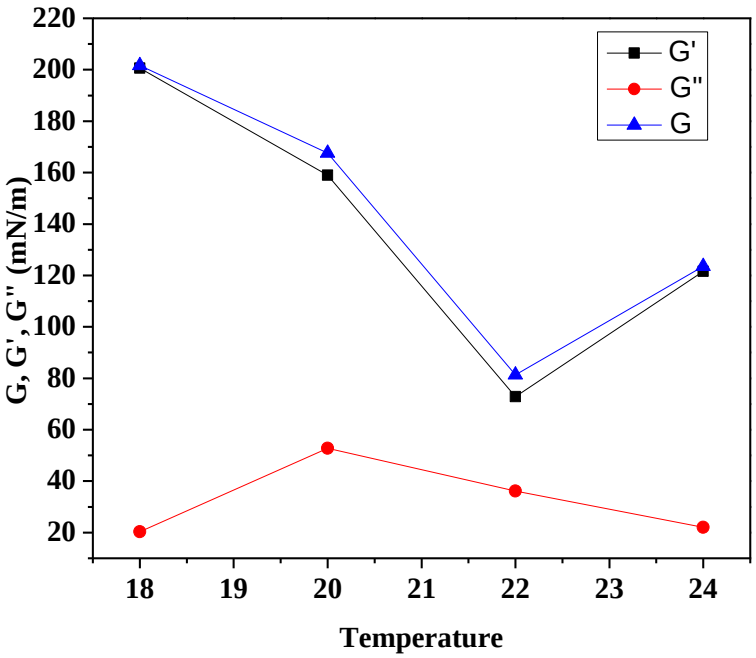

Figure 4.10 Variation of G, G', G" with subphase temperatures.

The subphase temperature 18^0C is selected as the final temperature for the deposition process as there value of dissipation is the least for this temperature and the value of Elastic modulus (G) and Storage modulus (G') is approximately equal as shown in figure 4.12.

Final dipping parameters: A complete characterization of the as synthesized PVDF Langmuir monolayers using static Π-A isotherms, hysteresis as well as the dynamic oscillating barrier techniques allows for us to determine the trough parameters for the most stable PVDF monolayer:

Compression rate: 25 mm/min

Temperature: 18˚C

Also all the depositions were started with the hydrophilic glass substrate already dipped in the subphase before the spreading of the PVDF monolayer. So, first movement of the dipper is always upstroke.

4.3 Deposition of PVDF Langmuir Blodgett films

The dipping parameters are optimized for the deposition of PVDF monolayers on a glass substrate. The dipping is started with an upstroke by dipping the substrate in the subphase before dispersing the monolayer. The up and down speed of the dipper is taken as 5 mm/min.

The transfer ratio (TR) at these conditions for seven cycles is shown in the figure 4.11 (a). The transfer ratio comes out to be very low because of the high dipping speed. The dipping speed is reduced to 3 mm/min for having sufficient transfer ratio. The corresponding plot is shown in figure 4.11 (b). The negative transfer ratio for the downstroke indicates that the film is getting dissolved in the subphase. In order to avoid this it was decided to test two possibilities:

a) the hold time in upstate has to be increased to dry out the film completely
b) the speed of downstroke has to be increased.

Effect of increasing the hold time: The hold time in upstate is increased to 5 min from 1 minute. This is done for proper drying of the deposited initial layer and hence reducing the possibility of dissolution. But this has no effect on the negative transfer ratio as can be seen in figure 4.11 (c). So the hold time is set back to 1 min for further depositions.

Effect of downstroke speed: The downstroke speed is further increased to 13 mm/min in order to give the previously deposited film very less time to dissolve in the subphase. The results are shown in figure 4.11 (d). This gives the somewhat less negative value of transfer ratio for alternate layers.

Effect of upstroke speed: In order to maximize the transfer ratio for the upstroke, the speed is decreased to 2 mm/min. The results are shown in figure 4.11 (e). This reducing of speed gives a significantly high value of transfer ratio.

The speed of downstroke was also increased to 15 mm/min for the last case. The value of transfer ratio obtained for the first upstroke at these final conditions is good enough for having the further deposition process. The deposition of monolayer takes place only for the upstroke and only a single layer is deposited at a time. After every single layer, the whole process of changing the subphase and dispersing a new monolayer is done for consecutive layers.

In this manner 1 layer was transferred on to glass, ITO coated glass and mica substrates. And the same were annealed for the final phase formation.

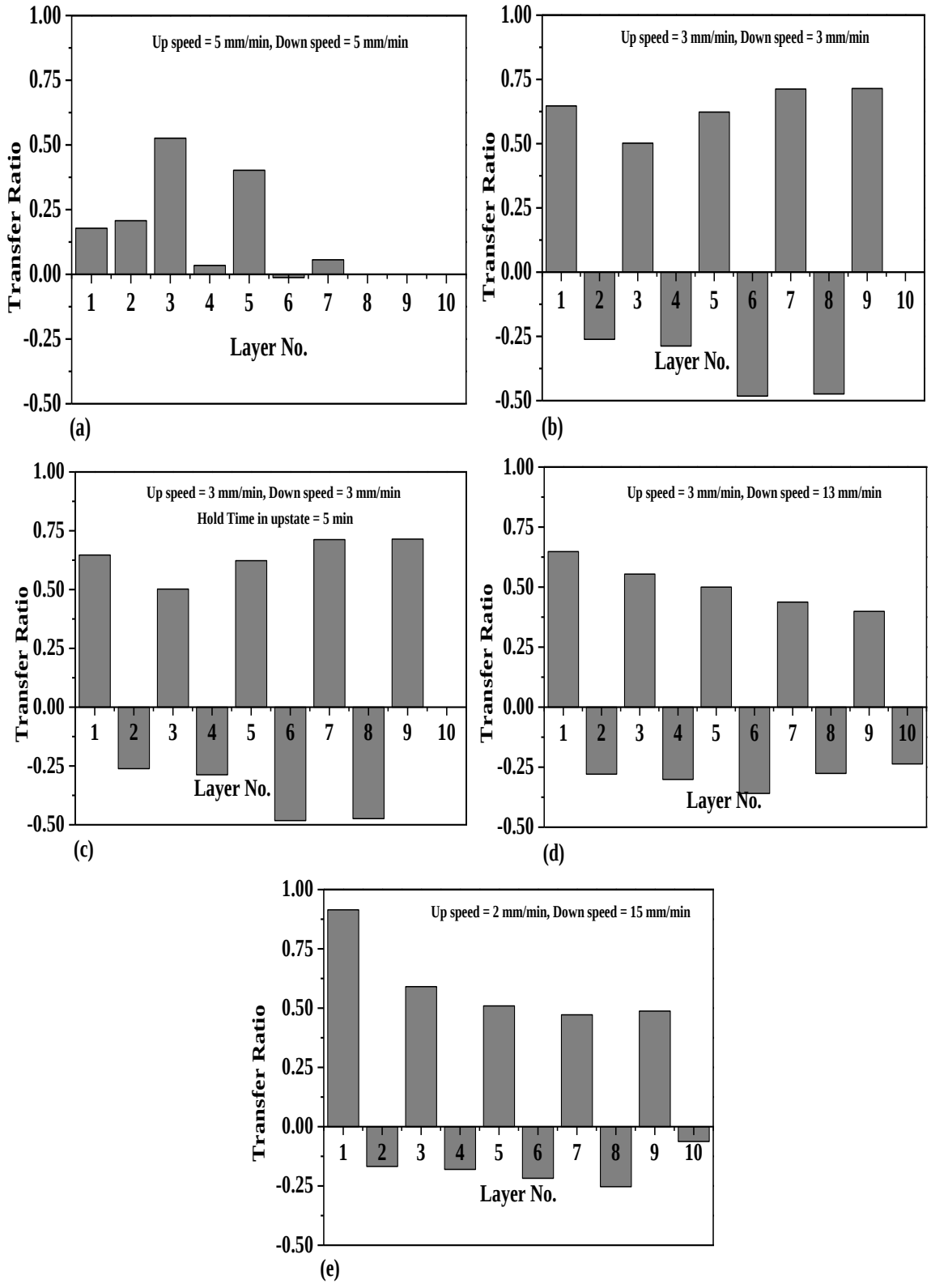

Figure 4.11 Variation of transfer ratio with layer number.

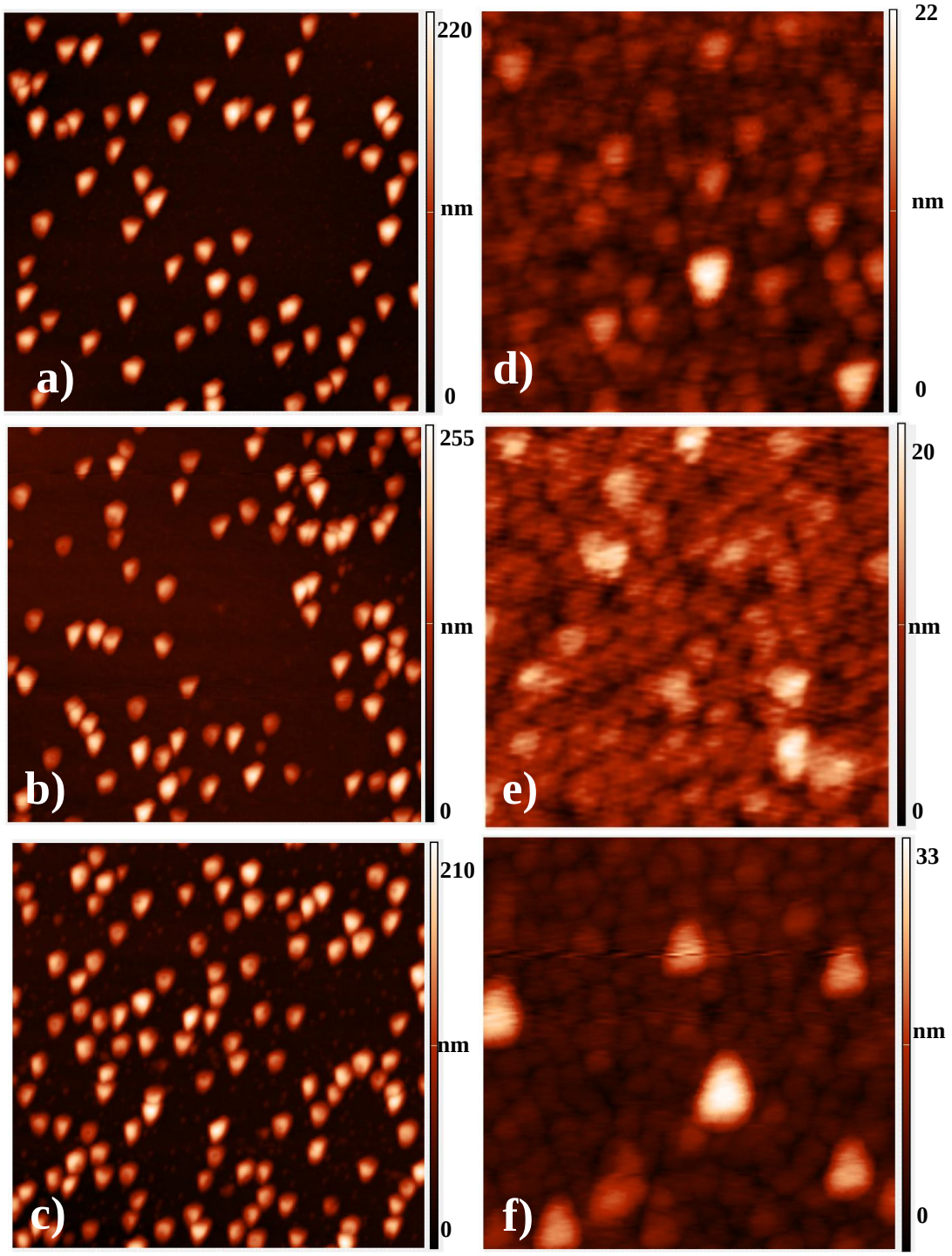

Figure 4.12 AFM images of single layer annealed PVDF LB films. Large area scans (10μm ×10μm) for a) mica, b) Glass, c) ITO coated glass. Small area scans (1μm ×1μm) for d) mica, e) Glass, f) ITO coated glass.

4.4 Atomic Force Microscopy (AFM)

The PVDF LB films formed were characterized topographically after the β-phase formation using AFM to understand the effect of the substrates. All the three substrates used are hydrophilic with their roughness varying as: Mica < Glass <ITO coated glass. Figure 4.12 shows the large and small scan size images for the 3 films. The images clearly show that the final films are rough due to the growth of crystallites on the film surface.

The roughness analysis data shows that even though the film for the atomically smooth Mica substrate seems smoother but its rms roughness is comparable to that deposited on glass (Table 4.8). An interesting result to emerge from this data was that even though the rms roughness of the film deposited on the ITO coated substrate is similar as that for the other substrates at larger scale but the small scale roughness is nearly double. This indicates that the film characteristics are controlled by the substrate roughness but in the current set of samples the crystallite growth on the surface is overshadowing the effect.

Table 4.8 r.m.s. Roughness for different substrates.

Substrate	**r.m.s. Roughness (nm)**	
	Large scan	Small Scan
Mica	42.6	2.5
Glass	42.8	2.5
ITO	43.5	5.0

Chapter 5

Conclusion and future possibilities

5.1 Conclusion

NMP (polar aprotic solvent) was used as solvent for PVDF. To obtain good transfer characteristics the PVDF monolayers on the water surface were characterized for different compression rates and subphase temperature. The isotherm, hysteresis and barrier oscillation experiments show that the most stable PVDF films were obtained at18 ˚C for 25 mm/min compression rate. Hysteresis isotherms results were especially important since they show that the monolayers formed at the compression rate of 25 mm/min are most stable with very small MMA or elasticity change in successive cycles. Thin films of PVDF were deposited on various substrates using the LB technique. Variation of the dipping parameters brought to fore the dissolving nature of the PVDF film during the down stroke. It became apparent that the LB films can be transferred only for the upstroke motion, one at a time. The process of changing the subphase and dispersing the monolayers was done after every layer. The topographic analysis of the final films shows the emergence of few crystallites on the film surface which makes the films rough and overshadows the effect on film topography due to substrate.

5.2 Future scope

The LB deposited PVDF films should be studied further to understand the effect of annealing temperature and time on the topography of the final films. The films deposited on the ITO coated substrate should be analysed further for ferroelectric properties.